bioRxiv preprint doi: https://doi.org/10.1101/148809; this version posted June 14, 2017. The copyright holder for this preprint (which was not certified by peer review) is the author/funder, who has granted bioRxiv a license to display the preprint in perpetuity. It is made available under aCC-BY-NC-ND 4.0 International license.

1 **Reduced chlorhexidine and daptomycin susceptibility arises in vancomycin-resistant**
2 ***Enterococcus faecium* after serial chlorhexidine exposure**
3
4
5
6 Pooja Bhardwaj[a], Amrita Hans[a], Kinnari Ruikar[a], Ziqiang Guan[b] and Kelli L. Palmer[a]*
7
8 [a]Department of Biological Sciences, University of Texas at Dallas, Richardson, Texas, USA
9 [b]Department of Biochemistry, Duke University Medical Center, Durham, NC, USA
10
11
12
13
14 Running title: Chlorhexidine adaptation in *E. faecium*
15
16
17 *Corresponding author:
18
19 Email: kelli.palmer@utdallas.edu
20
21
22
23
24

bioRxiv preprint doi: https://doi.org/10.1101/148809; this version posted June 14, 2017. The copyright holder for this preprint (which was not certified by peer review) is the author/funder, who has granted bioRxiv a license to display the preprint in perpetuity. It is made available under aCC-BY-NC-ND 4.0 International license.

25 **Abstract**

26

27 Vancomycin-resistant *Enterococcus faecium* (VREfm) are critical public health concerns
28 because they are among the leading causes of hospital-acquired bloodstream infections.
29 Chlorhexidine (CHX) is a bisbiguanide cationic antiseptic that is routinely used for patient
30 bathing and other infection control practices. VREfm are likely frequently exposed to CHX;
31 however, the long-term effects of CHX exposure have not been studied in enterococci. In this
32 study, we serially exposed VREfm to increasing concentrations of CHX for a period of 21 days
33 in two independent experimental evolution trials. Reduced CHX susceptibility emerged (4-fold
34 shift in CHX MIC). Sub-populations with reduced daptomycin (DAP) susceptibility were
35 detected, which were further analyzed by genome sequencing and lipidomic analysis. Across
36 the trials, we identified adaptive changes in genes with predicted or experimentally confirmed
37 roles in chlorhexidine susceptibility (*efrE*), global nutritional stress response (*relA*), nucleotide
38 metabolism (*cmk*), phosphate acquisition (*phoU*), and glycolipid biosynthesis (*bgsB*), among
39 others. Moreover, significant alterations in membrane phospholipids were identified. Our results
40 are clinically significant because they identify a link between serial sub-inhibitory CHX exposure
41 and reduced DAP susceptibility. In addition, the CHX-induced genetic and lipidomic changes
42 described in this study offer new insights into the mechanisms underlying the emergence of
43 antibiotic resistance in VREfm.

44

45

46

bioRxiv preprint doi: https://doi.org/10.1101/148809; this version posted June 14, 2017. The copyright holder for this preprint (which was not certified by peer review) is the author/funder, who has granted bioRxiv a license to display the preprint in perpetuity. It is made available under aCC-BY-NC-ND 4.0 International license.

47 **Introduction**

48

49 *Enterococcus faecium* is a Gram-positive bacterium that naturally colonizes the human
50 gastrointestinal tract and is an opportunistic pathogen associated with bacteremia, urinary tract
51 infections, endocarditis, and wound infections (1-3). Vancomycin-resistant *E. faecium* (VREfm)
52 are of particular concern for infection treatment. VREfm are among the primary etiological
53 agents of central line-associated bloodstream infections (CLABSIs), a type of healthcare-
54 associated infection (HAI) that arises from central venous catheter use and is associated with
55 high mortality in the United States (4, 5). *E. faecium* contamination on indwelling venous
56 catheters, surgical instruments, and hospital surfaces is challenging to eradicate (2, 6-8). In
57 hospital and clinical settings, improper infection control practices, contaminated surfaces, and
58 indiscriminate use of antibiotics contribute to persistence of *E. faecium* (6, 9).

59

60 Chlorhexidine (CHX) is a cationic antiseptic and membrane-active antimicrobial (10-12). The
61 primary mechanism of action of CHX is to disrupt the bacterial cell membrane and cause
62 leakage of cytoplasmic contents and precipitation of cytoplasm (13-15). CHX is recommended
63 by the Society for Healthcare Epidemiology of America to reduce CLABSI occurrence in acute
64 care hospitals (16). Specifically, CHX bathing and CHX-impregnated cardiovascular catheters
65 are used for CLABSI control (16-18). Clinical reports have raised concerns about the long-term
66 effects of CHX bathing on hospital-associated pathogens (19-22). The CHX concentrations on
67 patient skin can fall below the MIC for VREfm between bathings (22). Frequent exposure to sub-
68 inhibitory CHX could select for VREfm mutants with reduced susceptibility to CHX and other
69 antimicrobials that also interact with the bacterial cell surface. It was recently reported that
70 colistin resistance emerged in the Gram-negative pathogen *Klebsiella pneumoniae* after
71 exposure to CHX (23).

72

bioRxiv preprint doi: https://doi.org/10.1101/148809; this version posted June 14, 2017. The copyright holder for this preprint (which was not certified by peer review) is the author/funder, who has granted bioRxiv a license to display the preprint in perpetuity. It is made available under aCC-BY-NC-ND 4.0 International license.

73 In a previous study, we used RNA sequencing to study the global transcriptomic responses of a
74 VanA-type VREfm strain to CHX (24). We found that CHX exposure elicited expression of
75 genes associated with antibiotic resistance and extracytoplasmic stress, including genes
76 associated with vancomycin resistance (*vanHAX*) and reduced daptomycin (DAP) susceptibility
77 (*liaXYZ*) (24). In the current study, we test the hypothesis that serial exposure to sub-MIC CHX
78 selects for VREfm mutants with reduced susceptibilities to CHX and other membrane and cell
79 wall-targeting antimicrobials, with particular focus on DAP.
80
81 **Materials and Methods**
82
83 **Bacterial strains and growth conditions**. Bacterial strains used in this study are shown in
84 Table 1. *E. faecium* was cultured at 37°C on brain heart infusion (BHI) agar or in BHI broth
85 without agitation unless otherwise stated. Unless otherwise stated, the CHX product used for
86 experiments was Hibiclens (4% wt/vol chlorhexidine gluconate with 4% isopropyl alcohol).
87 Chloramphenicol was used at 15 μg/ml for *E. coli* and *E. faecium*.
88
89 **Routine molecular biology techniques**. *E. faecium* genomic DNA (gDNA) was isolated using
90 a previously published protocol (25). DNA fragments were purified using the Purelink PCR
91 purification kit (Thermo Fisher). *Taq* polymerase (New England Biolabs; NEB) was used for
92 routine PCR. Routine DNA sequencing was performed by the Massachusetts General Hospital
93 DNA core facility (Boston, MA). Primers used are shown in Table S1.
94
95 **MIC determinations**. Vancomycin, ampicillin, and CHX MICs were determined by broth
96 microdilution in BHI as described previously (24). CHX MICs were recorded at 48 hr post-
97 inoculation. DAP MICs were measured using Etest (BioMérieux, Inc.) strips on Mueller-Hinton
98 agar (MHA) plates per the manufacturer's instructions. MICs were independently assessed at

bioRxiv preprint doi: https://doi.org/10.1101/148809; this version posted June 14, 2017. The copyright holder for this preprint (which was not certified by peer review) is the author/funder, who has granted bioRxiv a license to display the preprint in perpetuity. It is made available under aCC-BY-NC-ND 4.0 International license.

99 least three times.

100

101 **Quantitative RT-PCR (RT-qPCR).** *E. faecium* 1,231,410 (*E. faecium* 410) and 1,141,733
102 cultures treated for 15 min with 0X (control) and 1X MIC CHX were harvested and mixed with
103 two volumes of RNAProtect Bacteria reagent (Qiagen) according to the manufacturer's
104 recommendation and a previously published protocol (24). 100 ng RNA was used to synthesize
105 cDNA with Superscript II (Life Technologies) and 5 ng cDNA was used as template in RT-qPCR
106 with primers to amplify internal regions of *liaX* or *clpX*. Threshold cycle (C_T) values were used to
107 calculate the fold change of *liaX* gene expression between 1X MIC CHX-treated cultures and
108 control cultures (n=2 independent trials).

109

110 To assess *liaX* expression in the DAP mutants and the *E. faecium* 410 wild-type, overnight
111 cultures inoculated from glycerol stocks were diluted into fresh pre-warmed BHI. The cultures
112 were incubated at 37°C until an optical density at 600 nm (OD_{600}) of ~ 0.6 was reached. 15 ml of
113 the cultures were harvested as described above. The experiment was performed independently
114 three times and one-tailed Student's *t* test was used to assess significance.

115

116 **Serial passage experiments.** *E. faecium* 410 wild-type was used for *in vitro* serial passage
117 according to a previously published protocol (26).The CHX 1X MIC value for *E. faecium* 410
118 was 4.9 µg/ml on day 1. For serial passage, overnight culture was adjusted to OD_{600} 0.1 and
119 exposed to CHX below, at, and above the MIC in BHI broth. The cultures were incubated at
120 37°C, and after 24 hr, the cultures with visible growth in the highest drug concentration were
121 used as inoculum for the next round of passaging on day 2. Again, the inoculum OD_{600} was
122 adjusted to 0.1, and cultures were exposed to CHX as described above. Passages were
123 performed for 21 days. The serial passage experiment was performed independently twice,
124 referred to as Experiments A and B. Cultures from the 22nd day of experiment A (referred to as

bioRxiv preprint doi: https://doi.org/10.1101/148809; this version posted June 14, 2017. The copyright holder for this preprint (which was not certified by peer review) is the author/funder, who has granted bioRxiv a license to display the preprint in perpetuity. It is made available under aCC-BY-NC-ND 4.0 International license.

125 Population A) and experiment B (referred to as Population B) were analyzed in this study. *E.*
126 *faecium* 410 cultures were also passaged in BHI without CHX for 21 days in two independent
127 trials. Populations from the 21st day of these trials are referred to as 410-P1 and P2 in this
128 study.
129
130 **Agar daptomycin susceptibility assay.** Cultures of Population A and Population B were
131 inoculated directly from glycerol stocks into BHI broth and incubated overnight. Cultures were
132 serially diluted in 1X phosphate buffered saline (PBS) and spotted on MHA plates supplemented
133 with calcium (50 µg/ml) with or without 10 µg/ml DAP. Plates were incubated for 24-36 hr at
134 37°C prior to colony counting. Three (for Population A) or four (for Population B) independent
135 trials were performed. One-tailed Student's *t* test was used to assess significance. *E. faecium*
136 410 unpassaged (7 trials) and no-drug passaged populations (3 trials each) were assayed as
137 controls. Colonies arising on DAP plates from two independent trials each for Populations A and
138 B were pooled, inoculated in BHI broth, and cryopreserved.
139
140 **Genome sequencing and analysis.** Genomic DNA was isolated from overnight broth cultures.
141 DAP MIC was confirmed for these cultures by Etest assay. Library preparation and 2x150
142 paired end Illumina sequencing was performed by Molecular Research LP (Shallowater, Texas).
143 The *E. faecium* 410 wild-type strain was also sequenced as a control. Sequence reads were
144 first assembled to the previously published *E. faecium* 410 draft genome sequence
145 (NZ_ACBA00000000.1) using default parameters for local alignment in CLC Genomics
146 Workbench (Qiagen). Polymorphisms in the read assemblies were detected using the basic
147 variant mapping tool for sites with ≥10-fold coverage. Variations occurring with ≥50% frequency
148 were compared with the *E. faecium* 410 wild-type read assembly to find mutant-specific SNPs.
149 To detect putative transposon hops, the read mapping parameters were changed to global
150 instead of local alignment, and regions of interest were manually analyzed. ≥98.8% of

bioRxiv preprint doi: https://doi.org/10.1101/148809; this version posted June 14, 2017. The copyright holder for this preprint (which was not certified by peer review) is the author/funder, who has granted bioRxiv a license to display the preprint in perpetuity. It is made available under aCC-BY-NC-ND 4.0 International license.

151 nucleotide positions in the *E. faecium* 410 reference were covered ≥10-fold and included in
152 variation analyses. Variants unique to the DAP-resistant mutants were confirmed by Sanger
153 sequencing.
154
155 **Phosphate assay.** A commercially available kit (Sigma MAK030) and a previously published
156 protocol (27) were utilized to measure intracellular inorganic phosphate (P_i) levels. Overnight
157 cultures were diluted to an OD_{600} 0.01 in 50 ml pre-warmed BHI and incubated at 37°C with
158 shaking at 100 rpm. The phosphate levels were measured at four time points, time point 1:
159 OD_{600} 0.4 to 0.5; 2, OD_{600} 0.5 to 0.6; 3, OD_{600} 0.6 to 0.7; 4, OD_{600} 0.7 to 0.8. For each timepoint,
160 100 µl culture was serially diluted in 0.9% sterile NaCl and spotted on BHI plates for CFU
161 determination. Also, 1 ml of the culture was incubated on ice for 5 min and then pelleted at
162 13,300 X g for 2 min at 4°C. The pellet was washed twice in 1 ml double-distilled water,
163 resuspended in 0.5 ml double-distilled water, and then disrupted thrice (Fast-Prep-24; MPBio) at
164 6.5 m/s for 30 s. The homogenized samples were centrifuged at 13,300 X *g* for 15 min at 4°C.
165 Twenty-five µl of the supernatant was diluted with 25 µl double distilled water, and the P_i levels
166 were measured per the manufacturer's instructions. The phosphate levels were normalized by
167 CFU. One-tailed Student's *t* test was used to assess significance from three independent trials.
168
169 **Bacterial growth curves.** Overnight cultures from glycerol stocks were diluted to an OD_{600} 0.01
170 in 50 ml pre-warmed BHI and incubated at 37°C and shaking at 100 rpm. The OD_{600} values
171 were measured for 6 hr. The experiment was performed independently three times and one-
172 tailed Student's *t* test was used to assess significance.
173
174 **Rifampin resistance frequency.** Overnight cultures of *E. faecium* 410 wild-type and DAP-
175 resistant mutants were serially diluted in 1X PBS and spot-plated on BHI agar to obtain total
176 CFU counts. Three ml of the cultures were pelleted and spread on BHI agar plates

bioRxiv preprint doi: https://doi.org/10.1101/148809; this version posted June 14, 2017. The copyright holder for this preprint (which was not certified by peer review) is the author/funder, who has granted bioRxiv a license to display the preprint in perpetuity. It is made available under aCC-BY-NC-ND 4.0 International license.

177 supplemented with 50 µg/ml rifampin to obtain rifampin-resistant CFU counts. Plates were
178 incubated for 24-48 hr. Four independent trials were performed and the significance value was
179 calculated using one-tailed Student's *t* test.
180
181 **Gene deletion and complementation.** Loci (EFTG_02287-02288) encoding the predicted ABC
182 transport system EfrEF were deleted in-frame utilizing plasmid pHA101. Briefly, 999 bp flanking
183 upstream and downstream regions of the genes of interest were amplified using primers in
184 Table S1 and ligated with the plasmid pHA101, and propagated in *E. coli* EC1000. The
185 construct, pPB301, was sequence-verified and electroporated into *E. faecium* 410 using a
186 previously published protocol (24). Temperature shift at non-permissible temperature of 42°C
187 and counter-selection with p-chlorophenylalanine was followed according to a previously
188 published protocol (28). Deletion of EFTG_02287-02288 in the mutant strain (*E. faecium*
189 PB301) was confirmed by Sanger sequencing. For complementing this deletion *in trans*,
190 EFTG_02287-02288 with their putative native promoter were amplified and ligated with pLZ12
191 (29). The complementation construct (pAH201) was sequence-verified and electroporated into
192 the deletion mutant to generate the strain AH102. The empty pLZ12 plasmid was also
193 transformed into the deletion mutant as a control (strain AH101).
194
195 **Complementation assay for CHX susceptibility.** Overnight cultures of AH101 and AH102
196 were serially diluted and spot plated on BHI-chloramphenicol (15 µg/ml) plates supplemented
197 with or without 1/8X MIC CHX. The plates were incubated at 37°C for 24-36 hr. The CFU/ml of
198 three independent trials was quantified and one-tailed Student's *t* test was used to assess
199 significance.
200
201 **Lipidomic analysis.** Overnight cultures from the glycerol stock were inoculated into 10 ml BHI
202 and incubated at 37°C. The 10 ml cultures were added to pre-warmed 250 ml BHI and

bioRxiv preprint doi: https://doi.org/10.1101/148809; this version posted June 14, 2017. The copyright holder for this preprint (which was not certified by peer review) is the author/funder, who has granted bioRxiv a license to display the preprint in perpetuity. It is made available under aCC-BY-NC-ND 4.0 International license.

203 incubated until an OD_{600} of ~ 0.6 was obtained. 100 µl was removed for DAP Etest testing on
204 MHA plates. Also, 15 ml of the cultures was added to 2 volumes of RNAProtect Bacteria
205 reagent (Qiagen) according to manufacturer's recommendation and a previously published
206 protocol (24), and samples were used to assess *cls*, *cmk*, *clpX* or *liaX* expression by RT-qPCR
207 as described above. The remaining culture was pelleted at 10,000 rpm at 4°C. Cell pellets were
208 stored at -80°C prior to lipid extraction by the Bligh and Dyer method (30). Lipid analysis by
209 normal phase LC-electrospray ionization (ESI) MS was performed using an Agilent 1200
210 Quaternary LC system coupled to a high resolution TripleTOF5600 mass spectrometer (Sciex,
211 Framingham, MA), as previously described (31, 32). Normal phase LC was performed on an
212 Agilent 1200 Quaternary LC system using an Ascentis Silica HPLC column, (5 µm; 25 cm x 2.1
213 mm; Sigma-Aldrich). Mobile phase A and B solvents, flow conditions, and instrumental settings
214 for ESI/MS and MS/MS are as previously published (33). Data analysis was performed using
215 Analyst TF1.5 software (Sciex, Framingham, MA).

216

217 **Accession number.** Raw Illumina sequencing reads generated in this study is available in the
218 SRA under the accession number SRP108331.

219

220 **Results**

221

222 ***In vitro* evolution of reduced CHX susceptibility in VREfm.** Previous RNA sequencing
223 analysis identified up to 118-fold up-regulation of *liaXYZ* in CHX-treated *E. faecium* 1,231,410
224 (*E. faecium* 410) (24), a VanA-type vancomycin- and ampicillin-resistant blood isolate and
225 member of the hospital-adapted Clade A1 (34, 35). This was of interest because *liaXYZ* is
226 protective against DAP (26, 36-40). We confirmed the CHX-stimulated up-regulation of *liaX* in *E.*
227 *faecium* 410 and a commensal Clade B strain, *E. faecium* 1,141,733 (35) using RT-qPCR (Fig.
228 S1).

bioRxiv preprint doi: https://doi.org/10.1101/148809; this version posted June 14, 2017. The copyright holder for this preprint (which was not certified by peer review) is the author/funder, who has granted bioRxiv a license to display the preprint in perpetuity. It is made available under aCC-BY-NC-ND 4.0 International license.

229

230 We hypothesized that repeat exposure to sub-inhibitory CHX could select for mutants with
231 reduced susceptibility to CHX and concomitant reduced susceptibility to other antimicrobials. To
232 test this, we performed *in vitro* serial passaging of *E. faecium* 410 with CHX for a period of 21
233 days, starting with a sub-MIC concentration of 2.9 µg/ml (Fig. 1). Similar patterns of MIC shifts
234 were observed for two independent trials over the course of 21 days. The CHX MICs of the
235 evolved populations (referred to as populations A and B) recovered after one drug-free passage
236 was confirmed to be increased (19.6 µg/ml) as compared to the parental strain (Table 2). The
237 CHX MIC was not altered in *E. faecium* 410 passaged for 21 days in medium without CHX. We
238 conclude that reduced CHX susceptibility emerges in VREfm after serial *in vitro* CHX exposure.

239

240 The populations A and B had variable but significantly higher DAP MICs relative to the wild-type
241 strain (Table 2), with the DAP MIC in some experimental trials meeting the ≥ 4 µg/ml breakpoint
242 for DAP resistance (41). Vancomycin MIC was 2-fold higher for both populations relative to wild-
243 type, and ampicillin MIC was 2-fold higher for population A.

244

245 **Reduced DAP susceptibility is present in the CHX-passaged populations.** We sought to
246 further quantify and investigate the basis for elevated DAP MIC in the CHX-passaged
247 populations. The CHX-passaged populations (A and B) were cultured on agar with and without
248 10 µg/ml DAP to quantify CFU (Fig. 2). *E. faecium* 410 wild-type stock cultures (410-1 and -2)
249 and *E. faecium* 410 passaged for 21 days in the absence of CHX (410-P1 and -P2) were used
250 as controls. Sub-populations with reduced DAP susceptibility were detected in the CHX-
251 passaged populations (Fig. 2).

252

253 Next, isolated colonies arising on DAP plates from each of two independent DAP plating trials
254 were pooled and stocked for further analysis. These mutants will be referred to as DAP-A1 and

bioRxiv preprint doi: https://doi.org/10.1101/148809; this version posted June 14, 2017. The copyright holder for this preprint (which was not certified by peer review) is the author/funder, who has granted bioRxiv a license to display the preprint in perpetuity. It is made available under aCC-BY-NC-ND 4.0 International license.

255 DAP-A2 (from population A; 14 and 11 colonies were pooled, respectively) and DAP-B1 and
256 DAP-B2 (from population B; 18 and 5 colonies were pooled, respectively) hereafter. The DAP
257 MICs of these mutants after two DAP-free passages were found to be variable but significantly
258 higher than the *E. faecium* 410 wild-type (Table 2). The DAP mutants, with the exception of
259 DAP-B2, have significantly longer generation times than *E. faecium* 410 wild-type in BHI broth
260 (Table S2). No significant differences in spontaneous rifampin resistance frequencies were
261 observed between the DAP mutants and *E. faecium* 410 wild-type (Table S2), indicating that
262 these strains are not hyper-mutators. RT-qPCR analysis identified a small but statistically
263 significant increase in *liaX* expression in the DAP-A1 and A2 mutants relative to wild-type. The
264 increase was insignificant for DAP-B1 and B2 (Fig. S2).
265
266 **DAP strains have mutations in genes previously associated with reduced antimicrobial**
267 **susceptibilities.** Genome sequencing identified mutations occurring in the DAP strains relative
268 to *E. faecium* 410 wild-type (Table 3). All four share a common mutation in *efrE* (EFTG_02287),
269 which encodes one subunit of the heterodimeric ABC transporter EfrEF (42). *efrE* is up-
270 regulated 22-fold by *E. faecium* 410 in response to CHX (24), and deletion of *efrE* from *E.*
271 *faecalis* OG1RF confers increased susceptibility to CHX (43, 44). No mutations other than in
272 *efrE* were common to all strains.
273
274 DAP-A1 and DAP-A2 share IS*1251* insertions in the promoter region of *cmk*, which encodes
275 cytidylate kinase (Table 3). RT-qPCR confirmed the down-regulation of *cmk* in DAP-A2 in the
276 two trials but not in DAP-A1 (Fig. S3). Population heterogeneity in regards to IS*1251* insertion at
277 the *cmk* promoter was observed in DAP-A1 by gel electrophoresis analysis of *cmk* promoter
278 amplicons (data not shown).
279
280 DAP-A1 and DAP-A2 each have different mutations in *relA* and in a gene encoding a predicted

bioRxiv preprint doi: https://doi.org/10.1101/148809; this version posted June 14, 2017. The copyright holder for this preprint (which was not certified by peer review) is the author/funder, who has granted bioRxiv a license to display the preprint in perpetuity. It is made available under aCC-BY-NC-ND 4.0 International license.

281 alpha/beta hydrolase (Table 3). Production of (p)ppGpp, a bacterial alarmone, is controlled by
282 RelA. Changes in ppGpp concentration modulate the stringent stress response and impact
283 antibiotic tolerance and virulence in *Enterococcus* (45, 46). Mutations in *relA* have previously
284 been associated with *in vitro* (47) and *in vivo* (48) emergence of DAP resistance in *Bacillus*
285 *subtilis* and *E. faecium*, respectively. In DAP-A1, deletion of 11 bases (CTAGGATTTAC) from
286 *relA* results in synthesis of a truncated, 505 amino acid protein that lacks the C-terminal ACT
287 regulatory domain. The function of ACT domain as suggested is that it regulates the catalytic
288 activities of the amino terminal domain to ensure that synthesis and degradation of ppGpp are
289 not co-stimulated (49, 50). In DAP-A2, the A58E substitution is predicted by EMBOSS (51) to
290 convert a beta-strand fold into an alpha helix in the HD4 metal-dependent phosphohydrolase
291 domain of RelA. DAP-A1 and DAP-A2 also possess nonsense and frameshift mutations,
292 respectively, in a gene encoding a predicted alpha/beta hydrolase. To our knowledge, this gene
293 has not previously been linked with antimicrobial susceptibility.
294
295 Different mutations were identified in DAP-B1 and DAP-B2. In DAP-B1, a E61K substitution
296 occurs in PhoU. PhoU regulates phosphate intake by high-affinity inorganic phosphate-specific
297 transporters (*pst* transporters encoded by EFTG_01170-74 in *E. faecium*) in *E. coli* (52-56).
298 The *pst* transport system is up-regulated in *Streptococcus pneumoniae* in response to penicillin
299 (57), and mutations in the *pst* system led to decreased accumulation of reactive oxygen species
300 after exposure to penicillin (58). Moreover, an adaptive point mutation in a putative phosphate
301 transporter gene (*pitA*) in *S. aureus* conferred growth phase-dependent tolerance to DAP (27).
302 However, the exact molecular mechanism(s) of how inorganic phosphate levels alter
303 susceptibility to these antimicrobials is unclear. We confirmed that inorganic phosphate
304 concentrations were significantly lower in the DAP-B1 mutant relative to the wild-type for two of
305 four time-points assayed (Fig. S4).
306

bioRxiv preprint doi: https://doi.org/10.1101/148809; this version posted June 14, 2017. The copyright holder for this preprint (which was not certified by peer review) is the author/funder, who has granted bioRxiv a license to display the preprint in perpetuity. It is made available under aCC-BY-NC-ND 4.0 International license.

307 In DAP-B2, a V57M substitution occurs in BgsB (59). BgsB, a glycosyltransferase (GT),
308 catalyzes the transfer of glucose from UDP-glucose to 1,2-diacylglycerol (DAG) forming 3-D-
309 glucosyl-1,2-diacylglycerol (MGlcDAG). Further, MGlcDAG is converted to diglucosyl DAG
310 (DGlcDAG) by BgsA (60). MGlcDAG and DGlcDAG are important glycolipids for cell membrane
311 fluidity and lipoteichoic acid (LTA) synthesis. Deletion of *bgsB* in *E. faecalis* 12030 led to a
312 complete loss of cell membrane glycolipids and affected the chain length of glycerol phosphate
313 polymer of LTA. It also led to 2-fold increased sensitivity to antimicrobial peptides (colistin and
314 polymixin B), and reduced virulence in a rat model of endocarditis (59, 61). Deletion of other cell
315 wall glycosyltransferases (*epaOX* and *epaI*) in *E. faecalis* enhances susceptibility to DAP (62)
316 through perturbations in the cell envelope. A role for GTs in the production of immature
317 polysaccharides, which prevented DAP binding, was suggested.

318

319 ***efrE* impacts CHX susceptibility.** Because *efrE* mutations were shared by all DAP strains, we
320 deleted the EfrEF transport system from *E. faecium* 410 to assess its role in CHX and DAP
321 susceptibility. Deletion of *efrEF* resulted in a 4-fold decrease in CHX MIC as compared to *E.*
322 *faecium* 410 (n=3 independent trials). The median DAP MIC of the Δ*efrEF* mutant was
323 determined to be 2 μg/ml (range, 2-3 μg/ml; n=5 independent trials; *p*-value = 0.09 compared to
324 *E. faecium* 410 wild-type using one-tailed Student's *t* test). Complementation *in trans* with *efrEF*
325 on a multi-copy vector (AH102) resulted in a 2- to 4-fold increase in CHX MIC as compared to
326 an empty vector control strain (AH101) using broth microdilution assays (n=2 independent
327 trials). However, we observed a growth inhibition effect when chloramphenicol was added to the
328 broth microdilution assay for vector selection. Hence, we utilized a spot-plating assay to quantify
329 CFU differences between strains AH101 and AH102 in the presence of CHX and
330 chloramphenicol (Fig. S5). Complementation of ABC transporter genes *in trans* resulted in
331 significant increase in CFU count in the presence of CHX compared to control cultures.

332

bioRxiv preprint doi: https://doi.org/10.1101/148809; this version posted June 14, 2017. The copyright holder for this preprint (which was not certified by peer review) is the author/funder, who has granted bioRxiv a license to display the preprint in perpetuity. It is made available under aCC-BY-NC-ND 4.0 International license.

333 To identify a putative function for EfrEF, we performed comparative lipidomic analysis of *E.*
334 *faecium* 410 and the *efrEF* deletion mutant. The most striking differences observed were for two
335 species whose positive ion $[M+H]^+$ signals are detected at m/z 288 and m/z 316 by ESI/MS.
336 These two species are present in *E. faecium* 410 wild-type, but absent in the *efrEF* deletion
337 mutant (Fig. S6). High resolution mass measurement and tandem MS analysis identified these
338 species as ethoxylated fatty amines previously identified as components of the anti-static
339 additive Atmer-163 (63) commonly used in consumer products such as plastics. The *m/z* 288
340 and 316 ions correspond to the $[M+H]^+$ ions of Atmer-163 containing C_{13} and C_{15} fatty alkyl
341 chains, respectively. The absence of Atmer-163 (C_{13}) and Atmer-16 (C_{15}) in the *efrEF* mutant
342 suggests that this ABC transporter is involved in transporting the Atmer-163 species, with lipid-
343 like structures, from media into the cells.
344

345 **Distinct alterations of membrane phospholipid compositions in DAP mutants.** We next
346 compared lipid profiles between the DAP mutants and *E. faecium* 410 wild-type. The lipid
347 extracts were subjected to normal phase LC-ESI/MS using a silica column for lipid separation.
348 As shown by the total negative ion chromatogram data in Fig. 3 and Table S3, cardiolipin
349 (bisphophatidylglycerol; CL), an anionic phospholipid, was dramatically reduced in DAP-A
350 mutants (10-fold in DAP-A1 and 12-fold in DAP-A2) as compared to *E. faecium* 410. As
351 expected, an increased accumulation of the precursor phosphatidic acid (PA) (4-fold in DAP-A1
352 and 5-fold in DAP-A2) was also detected. The expression levels of two predicted cardiolipin
353 synthase (*cls*) genes (EFTG_00614 and EFTG_01168), which mediate reversible
354 transphosphatidylation of PG molecules to synthesize cardiolipin, were not significantly altered
355 compared to *E. faecium* 410 (data not shown). In contrast to DAP-A mutants, CL and PA
356 contents were not significantly altered in DAP-B mutants (Table S3), suggesting that DAP-A and
357 DAP-B mutants do not share identical molecular mechanisms for reduced DAP susceptibility
358 despite their similar DAP phenotypes.

bioRxiv preprint doi: https://doi.org/10.1101/148809; this version posted June 14, 2017. The copyright holder for this preprint (which was not certified by peer review) is the author/funder, who has granted bioRxiv a license to display the preprint in perpetuity. It is made available under aCC-BY-NC-ND 4.0 International license.

359

360 Significant changes were observed in several other lipid species in DAP mutants. As shown in
361 Table S3, in DAP-B1, levels of GPDD (glycerolphosphate DGlcDAG), a LTA precursor, were
362 about 4-fold and lysylphosphaditylglycerol (LPG) were 4-fold higher than *E. faecium* 410 wild-
363 type. In DAP-B2, amounts of monoglucosyl DAG (MGlcDAG or MHDAG) were 2-fold higher,
364 potentially as a result of the *bgsB* mutation. The levels of GPDD were at least 2-fold higher for
365 all DAP-A and -B strains.

366

367 **Discussion**

368

369 The goal of this study was to test the hypothesis that serial exposure to sub-MIC CHX selects
370 for VREfm mutants with reduced susceptibilities to CHX, with concomitant effects on
371 susceptibility to other membrane and cell wall-targeting antimicrobials. Our serial passage
372 experiments demonstrate that reduced CHX susceptibility can emerge in VREfm after repeat
373 sub-inhibitory exposure. Moreover, our DAP plating experiments demonstrate that reduced DAP
374 susceptibility concomitantly emerges in a sub-population of CHX-passaged cells. Using
375 genomics and lipidomics, we identified genetic and physiological changes occurring in these
376 sub-populations with reduced DAP susceptibility.

377

378 CHX, a cationic antiseptic, interacts with the bacterial cell membrane (12). Various mechanisms
379 of reduced CHX susceptibility in Gram-negative and -positive bacteria have been reported. The
380 two main mechanisms include CHX efflux (23, 42-44, 64-67) and changes in outer membrane
381 content (68, 69). The recently identified two-component system ChtRS contributes to CHX
382 tolerance in *E. faecium*, presumably via regulation of expression of genes in its regulon, which is
383 currently undefined (70). In this study, we have confirmed a role for the heterodimeric ABC
384 transporter in CHX susceptibility in VREfm. Deletion of *efrEF* increases susceptibility of *E.*

bioRxiv preprint doi: https://doi.org/10.1101/148809; this version posted June 14, 2017. The copyright holder for this preprint (which was not certified by peer review) is the author/funder, who has granted bioRxiv a license to display the preprint in perpetuity. It is made available under aCC-BY-NC-ND 4.0 International license.

385 *faecium* 410 to CHX, and an amino acid substitution in EfrE is associated with decreased
386 susceptibility to CHX. The substrate of EfrEF was not assessed in prior studies. By lipidomic
387 analysis, we found that presence of two ethoxylated fatty amine fatty alkyl diethanolamine
388 compounds was abolished in the *efrEF* deletion mutant relative to wild-type. It remains to be
389 determined if these compounds are protective against CHX. Nonetheless, their lipid-like
390 structures may provide useful clues in identifying the molecular species that EfrEF transports, or
391 in the functional studies of EfrEF.
392
393 Daptomycin (DAP) is a cyclic lipopeptide antibiotic used to treat infections caused by multidrug-
394 resistant Gram-positive pathogens including VREfm (71-73). DAP resistance arises by mutation,
395 leading to treatment failure (74). DAP is a negatively charged molecule that requires calcium
396 ions for activity. Interaction of the cationic DAP-calcium complex with the membrane induces
397 daptomycin oligomerization, membrane phospholipid remodeling, and other physiological
398 alterations, ultimately leading to cell death (47, 75-79). Broadly speaking, alterations in cell
399 surface composition and in cellular stress responses are associated with reduced DAP
400 susceptibility in Gram-positive bacteria (80, 81).
401
402 In this study, we identified adaptive changes in genes with predicted or experimentally
403 confirmed roles in chlorhexidine susceptibility (*efrE*), global nutritional stress response (*relA*),
404 nucleotide metabolism (*cmk*), phosphate acquisition (*phoU*), and glycolipid biosynthesis (*bgsB*)
405 occurring in the CHX-passaged mutants with reduced DAP susceptibilities. That the strains
406 arising on DAP plates are not hyper-mutators indicates that these mutations arose as a result of
407 CHX selection. It remains to be determined at what point in the CHX serial passage
408 experiments reduced DAP susceptibility emerged, as only the beginning and end-points of the
409 evolution experiments were assessed in this study. Deep sequencing of populations at
410 beginning, mid- and end-points of the CHX passage experiments could be used in future studies

bioRxiv preprint doi: https://doi.org/10.1101/148809; this version posted June 14, 2017. The copyright holder for this preprint (which was not certified by peer review) is the author/funder, who has granted bioRxiv a license to display the preprint in perpetuity. It is made available under aCC-BY-NC-ND 4.0 International license.

411 to further examine the diversity and frequency of genetic variations arising as a result of serial
412 sub-inhibitory CHX exposure. Moreover, it remains to be determined whether susceptibility to
413 host-associated cationic antimicrobial peptides is also altered as a result of serial CHX
414 exposure.
415
416 Lipidomic analysis of the DAP mutants identified major alterations in membrane lipid
417 compositions, underscoring a link between membrane lipid compositions and DAP
418 susceptibility. CL, an anionic phospholipid, is present at the septal and polar regions in the
419 bacterial cell membrane and is important for the regulation of processes like cell division,
420 membrane transport, and localization of proteins to specific sites (82, 83). Since DAP
421 preferentially binds to charged regions of the membrane, we hypothesize that reduced amounts
422 of CL in DAP mutants from Population A can affect the binding of DAP antibiotic to the
423 membrane regions. Tran et al showed that remodeling of CL can divert DAP away from division
424 septum in *E. faecalis* (84). In Population B, we detected elevated levels of MHDAG and LTA
425 precursor, implying that LTA synthesis is impaired in these DAP strains. Zorko et al showed
426 direct binding and inhibition of LTA synthesis by CHX using fluorescence displacement and
427 isothermal titration (85). Another study showed inactivation of LTA by CHX in *E. faecalis* (86).
428 DAP mechanism of action by inhibition of LTA synthesis has also been suggested (87, 88) but
429 recent reports have not supported this mechanism (89, 90). In future studies, we will assess the
430 specific contributions of individual mutations identified in the DAP mutants to the lipid content
431 alterations observed.
432
433 Our work has clinical implications. If sub-inhibitory CHX exposure selects for VREfm mutants
434 with enhanced abilities to tolerate or resist DAP, these mutants could contribute to treatment
435 failures with DAP. Frequent improper use of CHX (i.e., presence of sub-inhibitory concentrations
436 on patient skin) may favor the emergence and persistence of these VREfm mutants in

bioRxiv preprint doi: https://doi.org/10.1101/148809; this version posted June 14, 2017. The copyright holder for this preprint (which was not certified by peer review) is the author/funder, who has granted bioRxiv a license to display the preprint in perpetuity. It is made available under aCC-BY-NC-ND 4.0 International license.

437 healthcare settings. Surveillance of VREfm from hospital wards utilizing CHX bathing would be
438 useful to monitor the long-term impact of CHX bathing on these organisms. Routine sub-
439 inhibitory CHX exposure may be a contributing factor to the clinical emergence of DAP
440 resistance in VREfm.
441
442 **Acknowledgements**
443
444 We would like to thank Dr. Ronda Akins for providing daptomycin. This work was supported by
445 start up funds from the University of Texas at Dallas to K.L.P. The MS facility in the Department
446 of Biochemistry at Duke University Medical Center and Z.G. were partially supported by grants
447 GM-069338 and EY023666 from the National Institutes of Health.
448

bioRxiv preprint doi: https://doi.org/10.1101/148809; this version posted June 14, 2017. The copyright holder for this preprint (which was not certified by peer review) is the author/funder, who has granted bioRxiv a license to display the preprint in perpetuity. It is made available under aCC-BY-NC-ND 4.0 International license.

449 **Table 1. Bacterial strains and plasmids used in the study.**
450

Strain or plasmid	Description	Reference
Bacterial strains		
E. faecium 1,231,410	Clade A skin and soft tissue infection isolate; VanA-type VRE, DAP-susceptible	(35)
E. faecium 1,141,733	Clade B clinical isolate, Van-susceptible	(35)
Population A	*In vitro* evolved population with reduced CHX susceptibility from Experiment A, stocked from 22nd Day	This study
Population B	*In vitro* evolved population with reduced CHX susceptibility from Experiment B, stocked from 22nd Day	This study
410-P1	*E. faecium* 410 *in vitro* evolved population in BHI from Day 21st, Trial 1	This study
410-P2	*E. faecium* 410 *in vitro* evolved population in BHI from Day 21st, Trial 2	This study
DAP-A1	Mutants with reduced DAP susceptibility from Population A; Trial 2	This study
DAP-A2	Mutants with reduced DAP susceptibility, from Population A; Trial 3	This study
DAP-B1	Mutants with reduced DAP susceptibility, from Population B; Trial 2	This study
DAP-B2	Mutants with reduced DAP susceptibility, from Population B; Trial 3	This study
PB301	*E. faecium* 410 ABC transporter (Eftg_02287-88) deletion mutant	This study
AH101	*E. faecium* 410 ABC transporter (Eftg_02287-88) deletion mutant transformed with empty pLZ12 plasmid	This study
AH102	*E. faecium* 410 ABC transporter (Eftg_02287-88) deletion transformed with pAH201 complementation plasmid	This study
E. coli EC1000	*E. coli* cloning host; provides *repA* in *trans; F$^-$ araD139* (*ara ABC-leu*)7679 *galU galK lacX74 rspL thi*; *repA* of pWV01 in *glgB*; Km	(91)
Plasmids		
pLZ12	*E. coli* and *Streptococcus* shuttle vector, confers chloramphenicol resistance (Cam^R)	(29)
pHA101	Markerless counter selectable exchange plasmid for *Enterococcus*, confers Cam^R	(24)
pAH201	pLZ12 plasmid containing a 4.186-kb BamHI/BamHI-fragment with ABC transporter genes (Eftg_02287-88) under its native promoter	This study
pPB301	pHA101 containing a 1.998-kb EcoRI/BamHI-digested fragment with flanking upstream and downstream of ABC transporter genes (Eftg_02287-88)	This study

bioRxiv preprint doi: https://doi.org/10.1101/148809; this version posted June 14, 2017. The copyright holder for this preprint (which was not certified by peer review) is the author/funder, who has granted bioRxiv a license to display the preprint in perpetuity. It is made available under aCC-BY-NC-ND 4.0 International license.

451

452 **Table 2. MIC values for CHX and cell wall-targeting antibiotics.**

Strain or Population	CHX MIC[a]	DAP MIC range, median (*p*-value)[b]	AMP MIC	VAN MIC
E. faecium 410	4.9	2, 2 (N/A)	195	250
Population A	19.6	2-6, 3 (0.0085)	390	500
Population B	19.6	3-4, 3.5 (0.0006)	195	500
DAP-A1	19.6	3-6, 4 (0.0043)	195	500
DAP-A2	19.6	3-6, 4 (0.0015)	390	1000
DAP-B1	19.6	3-4, 3.5 (0.0006)	195	1000
DAP-B2	19.6	3-4, 3.5 (0.0006)	195	1000

453

454 [a]All MICs in table expressed in µg/ml.
455 [b]DAP MICs were performed independently either 7 (for *E. faecium* 1,231,410 and Population A) or
456 6 times. The one-tailed unpaired Student's *t* test was used to assess significance of the difference
457 in MIC as compared to *E. faecium* 1,231,410. *E. faecium* 410, *E. faecium* 1,231,410; AMP,
458 ampicillin; Van, vancomycin.

Table 3. List of mutations identified by whole-genome sequencing in the DAP-resistant mutants.

Mutant	Description of gene	Nucleotide variation (frequency)[a]	Amino acid change	*E. faecalis* V583 ortholog
DAP-A1	Eftg_02287 ABC transporter	C67008T (98.47%)	Ala290Val	EF2226
	Eftg_01724 RelA/SpoT (*relA*)	CTAGGATTTAC30479Del (98.19%)	Leu505fs	EF1974
	Eftg_01135 Alpha/beta hydrolase	G137748A (55.64%)	Trp150*	EF1505
	Eftg_00577 Cytidylate kinase (*cmk*) promoter	A618699IS*1251*[b]	IS*1251* insertion	EF1547
DAP-A2	Eftg_02287 ABC transporter	C67008T (99.77%)	Ala290Val	EF2226
	Eftg_01724 RelA/SpoT (*relA*)	CA29139AG (95.74%)	Ala58Glu	EF1974
	Eftg_01135 Alpha/beta hydrolase	137847G insertion (88.17%)	Ile184fs	EF1505
	Eftg_00577 Cytidylate kinase (*cmk*) promoter	A618699IS*1251*[b]	IS*1251* insertion	EF1547
DAP-B1	Eftg_02287 ABC transporter	C67008T (98.962%)	Ala290Val	EF2226
	Eftg_01175 PhoU regulator	G173845A (99.61%)	Glu61Lys	EF1754
	Eftg_02534 Transposase	C71844A (99.47%)	Lys206Asn	
DAP-B2	Eftg_02287 ABC transporter	C67008T (99.36%)	Ala290Val	EF2226
	Eftg_02162 Glycosyltransferase (*bgsB)*	C50223T (67.09%)	Val57Met	EF2890

[a]Frequency of mutation in the read assembly as determined by variant detection in CLC Genomics Workbench.
[b]Precise location of insertion was mapped by Sanger sequencing.

bioRxiv preprint doi: https://doi.org/10.1101/148809; this version posted June 14, 2017. The copyright holder for this preprint (which was not certified by peer review) is the author/funder, who has granted bioRxiv a license to display the preprint in perpetuity. It is made available under aCC-BY-NC-ND 4.0 International license.

bioRxiv preprint doi: https://doi.org/10.1101/148809; this version posted June 14, 2017. The copyright holder for this preprint (which was not certified by peer review) is the author/funder, who has granted bioRxiv a license to display the preprint in perpetuity. It is made available under aCC-BY-NC-ND 4.0 International license.

459 **References cited**

460

461 1. **Agudelo Higuita NI, Huycke MM**. 2014. Enterococcal Disease, Epidemiology, and
462 Implications for Treatment. *In* Gilmore MS, Clewell DB, Ike Y, Shankar N (ed),
463 Enterococci: From Commensals to Leading Causes of Drug Resistant Infection, Boston.
464 2. **Arias CA, Murray BE**. 2012. The rise of the *Enterococcus*: beyond vancomycin
465 resistance. Nat Rev Microbiol **10**:266-78.
466 3. **Gilmore MS, Lebreton F, van Schaik W**. 2013. Genomic transition of enterococci from
467 gut commensals to leading causes of multidrug-resistant hospital infection in the
468 antibiotic era. Curr Opin Microbiol **16**:10-6.
469 4. **Sievert DM, Ricks P, Edwards JR, Schneider A, Patel J, Srinivasan A, Kallen A,**
470 **Limbago B, Fridkin S, et al.** 2013. Antimicrobial-resistant pathogens associated with
471 healthcare-associated infections: summary of data reported to the National Healthcare
472 Safety Network at the Centers for Disease Control and Prevention, 2009-2010. Infect
473 Control Hosp Epidemiol **34**:1-14.
474 5. **Centers for Disease Control and Prevention**. 2011. Vital signs: central line-associated
475 blood stream infections--United States, 2001, 2008, and 2009. MMWR Morb Mortal Wkly
476 Rep **60**:243-8.
477 6. **Muto CA, Jernigan JA, Ostrowsky BE, Richet HM, Jarvis WR, Boyce JM, Farr BM**,
478 Shea. 2003. SHEA guideline for preventing nosocomial transmission of multidrug-
479 resistant strains of *Staphylococcus aureus* and *Enterococcus*. Infect Control Hosp
480 Epidemiol **24**:362-86.
481 7. **Boyce JM**. 2007. Environmental contamination makes an important contribution to
482 hospital infection. J Hosp Infect 65 Suppl **2**:50-4.
483 8. **Weber DJ, Anderson D, Rutala WA**. 2013. The role of the surface environment in
484 healthcare-associated infections. Curr Opin Infect Dis **26**:338-44.

bioRxiv preprint doi: https://doi.org/10.1101/148809; this version posted June 14, 2017. The copyright holder for this preprint (which was not certified by peer review) is the author/funder, who has granted bioRxiv a license to display the preprint in perpetuity. It is made available under aCC-BY-NC-ND 4.0 International license.

485 9. **Hota B.** 2004. Contamination, disinfection, and cross-colonization: are hospital surfaces
486 reservoirs for nosocomial infection? Clin Infect Dis **39**:1182-9.
487 10. **Davies A.** 1973. The mode of action of chlorhexidine. J Periodontal Res Suppl **12**:68-75.
488 11. **Davies GE, Francis J, Martin AR, Rose FL, Swain G**. 1954. 1:6-Di-4'-
489 chlorophenyldiguanidohexane (hibitane); laboratory investigation of a new antibacterial
490 agent of high potency. Br J Pharmacol Chemother **9**:192-6.
491 12. **Koontongkaew S, Jitpukdeebodintra S**. 1995. Interaction of chlorhexidine with
492 cytoplasmic membranes of *Streptococcus mutans* GS-5. Caries Res **29**:413-7.
493 13. **Hugo WB, Longworth AR**. 1966. The effect of chlorhexidine on the electrophoretic
494 mobility, cytoplasmic constituents, dehydrogenase activity and cell walls of *Escherichia*
495 *coli* and *Staphylococcus aureus*. J Pharm Pharmacol **18**:569-78.
496 14. **Hugo WB, Longworth AR**. 1964. Some Aspects of the Mode of Action of Chlorhexidine.
497 J Pharm Pharmacol **16**:655-62.
498 15. **Hugo WB, Longworth AR**. 1965. Cytological Aspects of the Mode of Action of
499 Chlorhexidine Diacetate. J Pharm Pharmacol **17**:28-32.
500 16. **Marschall J, Mermel LA, Fakih M, Hadaway L, Kallen A, O'Grady NP, Pettis AM,**
501 **Rupp ME, Sandora T, Maragakis LL, Yokoe DS**, Society for Healthcare Epidemiology
502 of America. 2014. Strategies to prevent central line-associated bloodstream infections in
503 acute care hospitals: 2014 update. Infect Control Hosp Epidemiol **35**:753-71.
504 17. **Supple L, Kumaraswami M, Kundrapu S, Sunkesula V, Cadnum JL, Nerandzic MM,**
505 **Tomas M, Donskey CJ**. 2015. Chlorhexidine Only Works If Applied Correctly: Use of a
506 Simple Colorimetric Assay to Provide Monitoring and Feedback on Effectiveness of
507 Chlorhexidine Application. Infect Control Hosp Epidemiol **36**:1095-7.
508 18. **Rupp ME, Lisco SJ, Lipsett PA, Perl TM, Keating K, Civetta JM, Mermel LA, Lee D,**
509 **Dellinger EP, Donahoe M, Giles D, Pfaller MA, Maki DG, Sherertz R**. 2005. Effect of a
510 second-generation venous catheter impregnated with chlorhexidine and silver

bioRxiv preprint doi: https://doi.org/10.1101/148809; this version posted June 14, 2017. The copyright holder for this preprint (which was not certified by peer review) is the author/funder, who has granted bioRxiv a license to display the preprint in perpetuity. It is made available under aCC-BY-NC-ND 4.0 International license.

511 sulfadiazine on central catheter-related infections: a randomized, controlled trial. Ann
512 Intern Med **143**:570-80.
513 19. **Noto MJ, Wheeler AP**. 2015. Understanding chlorhexidine decolonization strategies.
514 Intensive Care Med **41**:1351-4.
515 20. **Noto MJ, Domenico HJ, Byrne DW, Talbot T, Rice TW, Bernard GR, Wheeler AP**.
516 2015. Chlorhexidine bathing and health care-associated infections: a randomized clinical
517 trial. JAMA **313**:369-78.
518 21. **Pittet D, Angus DC**. 2015. Daily chlorhexidine bathing for critically ill patients: a note of
519 caution. JAMA **313**:365-6.
520 22. **Popovich KJ, Lyles R, Hayes R, Hota B, Trick W, Weinstein RA, Hayden MK**. 2012.
521 Relationship between chlorhexidine gluconate skin concentration and microbial density
522 on the skin of critically ill patients bathed daily with chlorhexidine gluconate. Infect
523 Control Hosp Epidemiol **33**:889-96.
524 23. **Wand ME, Bock LJ, Bonney LC, Sutton JM**. 2017. Mechanisms of Increased
525 Resistance to Chlorhexidine and Cross-Resistance to Colistin following Exposure of
526 Klebsiella pneumoniae Clinical Isolates to Chlorhexidine. Antimicrob Agents Chemother
527 pii: e01162-16.
528 24. **Bhardwaj P, Ziegler E, Palmer KL.** 2016. Chlorhexidine Induces VanA-Type
529 Vancomycin Resistance Genes in Enterococci. Antimicrob Agents Chemother **60**:2209-
530 21.
531 25. **Adams HM, Li X, Mascio C, Chesnel L, Palmer KL**. 2015. Mutations associated with
532 reduced surotomycin susceptibility in *Clostridium difficile* and *Enterococcus* species.
533 Antimicrob Agents Chemother **59**:4139-47.
534 26. **Palmer KL, Daniel A, Hardy C, Silverman J, Gilmore MS**. 2011. Genetic basis for
535 daptomycin resistance in enterococci. Antimicrob Agents Chemother **55**:3345-56.
536 27. **Mechler L, Herbig A, Paprotka K, Fraunholz M, Nieselt K, Bertram R.** 2015. A novel

bioRxiv preprint doi: https://doi.org/10.1101/148809; this version posted June 14, 2017. The copyright holder for this preprint (which was not certified by peer review) is the author/funder, who has granted bioRxiv a license to display the preprint in perpetuity. It is made available under aCC-BY-NC-ND 4.0 International license.

537 point mutation promotes growth phase-dependent daptomycin tolerance in
538 *Staphylococcus aureus*. Antimicrob Agents Chemother **59**:5366-76.
539 28. **Thurlow LR, Thomas VC, Hancock LE**. 2009. Capsular polysaccharide production in
540 *Enterococcus faecalis* and contribution of CpsF to capsule serospecificity. J Bacteriol
541 **191**:6203-10.
542 29. **Perez-Casal J, Caparon MG, Scott JR.** 1991. Mry, a trans-acting positive regulator of
543 the M protein gene of *Streptococcus pyogenes* with similarity to the receptor proteins of
544 two-component regulatory systems. J Bacteriol **173**:2617-24.
545 30. **Bligh EG, Dyer WJ**. 1959. A rapid method of total lipid extraction and purification. Can J
546 Biochem Physiol **37**:911-7.
547 31. **Tan BK, Bogdanov M, Zhao J, Dowhan W, Raetz CR, Guan Z**. 2012. Discovery of a
548 cardiolipin synthase utilizing phosphatidylethanolamine and phosphatidylglycerol as
549 substrates. Proc Natl Acad Sci U S A **109**:16504-9.
550 32. **Li C, Tan BK, Zhao J, Guan Z.** 2016. In Vivo and in Vitro Synthesis of
551 Phosphatidylglycerol by an *Escherichia coli* Cardiolipin Synthase. J Biol Chem
552 **291**:25144-25153.
553 33. **Adams HM, Joyce LR, Guan Z, Akins RL, Palmer KL**. 2017. *Streptococcus mitis* and
554 *S. oralis* Lack a Requirement for CdsA, the Enzyme Required for Synthesis of Major
555 Membrane Phospholipids in Bacteria. Antimicrob Agents Chemother **61**.
556 34. **Palmer KL, Gilmore MS**. 2010. Multidrug-resistant enterococci lack CRISPR-*cas*. MBio
557 **1:**e00227-10.
558 35. **Palmer KL, Godfrey P, Griggs A, Kos VN, Zucker J, Desjardins C, Cerqueira G,
559 Gevers D, Walker S, Wortman J, Feldgarden M, Haas B, Birren B, Gilmore MS.**
560 2012. Comparative genomics of enterococci: variation in *Enterococcus faecalis*, clade
561 structure in *E. faecium*, and defining characteristics of *E. gallinarum* and *E. casseliflavus*.
562 MBio **3**:e00318-11.

bioRxiv preprint doi: https://doi.org/10.1101/148809; this version posted June 14, 2017. The copyright holder for this preprint (which was not certified by peer review) is the author/funder, who has granted bioRxiv a license to display the preprint in perpetuity. It is made available under aCC-BY-NC-ND 4.0 International license.

563 36. **Arias CA, Panesso D, McGrath DM, Qin X, Mojica MF, Miller C, Diaz L, Tran TT,**
564 **Rincon S, Barbu EM, Reyes J, Roh JH, Lobos E, Sodergren E, Pasqualini R, Arap**
565 **W, Quinn JP, Shamoo Y, Murray BE, Weinstock GM**. 2011. Genetic basis for *in vivo*
566 daptomycin resistance in enterococci. N Engl J Med **365**:892-900.
567 37. **Davlieva M, Shi Y, Leonard PG, Johnson TA, Zianni MR, Arias CA, Ladbury JE,**
568 **Shamoo Y**. 2015. A variable DNA recognition site organization establishes the LiaR-
569 mediated cell envelope stress response of enterococci to daptomycin. Nucleic Acids Res
570 **43**:4758-73.
571 38. **Davlieva M, Tovar-Yanez A, DeBruler K, Leonard PG, Zianni MR, Arias CA,**
572 **Shamoo Y**. 2016. An Adaptive Mutation in *Enterococcus faecium* LiaR Associated with
573 Antimicrobial Peptide Resistance Mimics Phosphorylation and Stabilizes LiaR in an
574 Activated State. J Mol Biol **428**:4503-4519.
575 39. **Diaz L, Tran TT, Munita JM, Miller WR, Rincon S, Carvajal LP, Wollam A, Reyes J,**
576 **Panesso D, Rojas NL, Shamoo Y, Murray BE, Weinstock GM, Arias CA**. 2014.
577 Whole-genome analyses of *Enterococcus faecium* isolates with diverse daptomycin
578 MICs. Antimicrob Agents Chemother **58**:4527-34.
579 40. **Miller C, Kong J, Tran TT, Arias CA, Saxer G, Shamoo Y**. 2013. Adaptation of
580 *Enterococcus faecalis* to daptomycin reveals an ordered progression to resistance.
581 Antimicrob Agents Chemother **57**:5373-83.
582 41. **Clinical and Laboratory Standards Institute (CLSI).** Performance Standards for
583 Antimicrobial Susceptibility Testing. **27th** ed. CLSI supplement M100, Wayne,
584 Pennsylvania 19087.
585 42. **Hurlimann LM, Corradi V, Hohl M, Bloemberg GV, Tieleman DP, Seeger MA**. 2016.
586 The Heterodimeric ABC Transporter EfrCD Mediates Multidrug Efflux in *Enterococcus*
587 *faecalis.* Antimicrob Agents Chemother **60**:5400-11.
588 43. **Davis DR, McAlpine JB, Pazoles CJ, Talbot MK, Alder EA, White C, Jonas BM,**

bioRxiv preprint doi: https://doi.org/10.1101/148809; this version posted June 14, 2017. The copyright holder for this preprint (which was not certified by peer review) is the author/funder, who has granted bioRxiv a license to display the preprint in perpetuity. It is made available under aCC-BY-NC-ND 4.0 International license.

589 **Murray BE, Weinstock GM, Rogers BL**. 2001. *Enterococcus faecalis* multi-drug
590 resistance transporters: application for antibiotic discovery. J Mol Microbiol Biotechnol
591 **3**:179-84.
592 44. **Davis DV, Rogers BL, White AC**. 2001. Multidrug resistance (mdr) efflux pump
593 polypeptides. Google Patents.
594 45. **Abranches J, Martinez AR, Kajfasz JK, Chavez V, Garsin DA, Lemos JA**. 2009. The
595 molecular alarmone (p)ppGpp mediates stress responses, vancomycin tolerance, and
596 virulence in *Enterococcus faecalis*. J Bacteriol **191**:2248-56.
597 46. **Gaca AO, Kajfasz JK, Miller JH, Liu K, Wang JD, Abranches J, Lemos JA**. 2013.
598 Basal levels of (p)ppGpp in *Enterococcus faecalis*: the magic beyond the stringent
599 response. MBio **4**:e00646-13.
600 47. **Hachmann AB, Sevim E, Gaballa A, Popham DL, Antelmann H, Helmann JD**. 2011.
601 Reduction in membrane phosphatidylglycerol content leads to daptomycin resistance in
602 *Bacillus subtilis*. Antimicrob Agents Chemother **55**:4326-37.
603 48. **Honsa ES, Cooper VS, Mhaissen MN, Frank M, Shaker J, Iverson A, Rubnitz J,**
604 **Hayden RT, Lee RE, Rock CO, Tuomanen EI, Wolf J, Rosch JW**. 2017. RelA Mutant
605 *Enterococcus faecium* with Multiantibiotic Tolerance Arising in an Immunocompromised
606 Host. MBio **8**:e00066-17.
607 49. **Mechold U, Murphy H, Brown L, Cashel M**. 2002. Intramolecular regulation of the
608 opposing (p)ppGpp catalytic activities of Rel(Seq), the Rel/Spo enzyme from
609 *Streptococcus equisimilis*. J Bacteriol **184**:2878-88.
610 50. **Hogg T, Mechold U, Malke H, Cashel M, Hilgenfeld R**. 2004. Conformational
611 antagonism between opposing active sites in a bifunctional RelA/SpoT homolog
612 modulates (p)ppGpp metabolism during the stringent response. Cell **117**:57-68.
613 51. **Rice P, Longden I, Bleasby A**. 2000. EMBOSS: the European Molecular Biology Open
614 Software Suite. Trends Genet **16**:276-7.

bioRxiv preprint doi: https://doi.org/10.1101/148809; this version posted June 14, 2017. The copyright holder for this preprint (which was not certified by peer review) is the author/funder, who has granted bioRxiv a license to display the preprint in perpetuity. It is made available under aCC-BY-NC-ND 4.0 International license.

615 52. **Nakata A, Amemura M, Shinagawa H.** 1984. Regulation of the phosphate regulon in
616 *Escherichia coli* K-12: regulation of the negative regulatory gene phoU and identification
617 of the gene product. J Bacteriol **159**:979-85.
618 53. **Muda M, Rao NN, Torriani A.** 1992. Role of PhoU in phosphate transport and alkaline
619 phosphatase regulation. J Bacteriol **174**:8057-64.
620 54. **Steed PM, Wanner BL.** 1993. Use of the rep technique for allele replacement to
621 construct mutants with deletions of the *pstSCAB-phoU* operon: evidence of a new role
622 for the PhoU protein in the phosphate regulon. J Bacteriol **175**:6797-809.
623 55. **Baek JH, Kang YJ, Lee SY.** 2007. Transcript and protein level analyses of the
624 interactions among PhoB, PhoR, PhoU and CreC in response to phosphate starvation in
625 *Escherichia coli*. FEMS Microbiol Lett **277**:254-9.
626 56. **Rice CD, Pollard JE, Lewis ZT, McCleary WR.** 2009. Employment of a promoter-
627 swapping technique shows that PhoU modulates the activity of the PstSCAB2 ABC
628 transporter in *Escherichia coli*. Appl Environ Microbiol **75**:573-82.
629 57. **Rogers PD, Liu TT, Barker KS, Hilliard GM, English BK, Thornton J, Swiatlo E,**
630 **McDaniel LS.** 2007. Gene expression profiling of the response of *Streptococcus*
631 *pneumoniae* to penicillin. J Antimicrob Chemother **59**:616-26.
632 58. **Fani F, Leprohon P, Legare D, Ouellette M.** 2011. Whole genome sequencing of
633 penicillin-resistant *Streptococcus pneumoniae* reveals mutations in penicillin-binding
634 proteins and in a putative iron permease. Genome Biol **12**:R115.
635 59. **Theilacker C, Sava I, Sanchez-Carballo P, Bao Y, Kropec A, Grohmann E, Holst O,**
636 **Huebner J.** 2011. Deletion of the glycosyltransferase *bgsB* of *Enterococcus faecalis*
637 leads to a complete loss of glycolipids from the cell membrane and to impaired biofilm
638 formation. BMC Microbiol **11**:67.
639 60. **Theilacker C, Sanchez-Carballo P, Toma I, Fabretti F, Sava I, Kropec A, Holst O,**
640 **Huebner J.** 2009. Glycolipids are involved in biofilm accumulation and prolonged

bioRxiv preprint doi: https://doi.org/10.1101/148809; this version posted June 14, 2017. The copyright holder for this preprint (which was not certified by peer review) is the author/funder, who has granted bioRxiv a license to display the preprint in perpetuity. It is made available under aCC-BY-NC-ND 4.0 International license.

641 bacteraemia in *Enterococcus faecalis*. Mol Microbiol **71**:1055-69.

642 61. **Haller C, Berthold M, Wobser D, Kropec A, Lauriola M, Schlensak C, Huebner J**.
643 2014. Cell-wall glycolipid mutations and their effects on virulence of *E. faecalis* in a rat
644 model of infective endocarditis. PLoS One **9**:e91863.

645 62. **Dale JL, Cagnazzo J, Phan CQ, Barnes AM, Dunny GM**. 2015. Multiple roles for
646 *Enterococcus faecalis* glycosyltransferases in biofilm-associated antibiotic resistance,
647 cell envelope integrity, and conjugative transfer. Antimicrob Agents Chemother **59**:4094-
648 105.

649 63. **Gonzalez-Rodriguez MV, Dopico-Garcia MS, Noguerol-Cal R, Carballeira-Amarelo**
650 **T, Lopez-Vilarino JM, Fernandez-Martinez G**. 2010. Application of liquid
651 chromatography in polymer non-ionic antistatic additives analysis. J Sep Sci **33**:3595-
652 603.

653 64. **Russell AD**. 2002. Introduction of biocides into clinical practice and the impact on
654 antibiotic-resistant bacteria. Symp Ser Soc Appl Microbiol **121**-135S.

655 65. **Costa SS, Viveiros M, Amaral L, Couto I**. 2013. Multidrug Efflux Pumps in
656 *Staphylococcus aureus*: an Update. Open Microbiol J **7**:59-71.

657 66. **Rajamohan G, Srinivasan VB, Gebreyes WA.** 2010. Novel role of *Acinetobacter*
658 *baumannii* RND efflux transporters in mediating decreased susceptibility to biocides. J
659 Antimicrob Chemother **65**:228-32.

660 67. **Hassan KA, Jackson SM, Penesyan A, Patching SG, Tetu SG, Eijkelkamp BA,**
661 **Brown MH, Henderson PJ, Paulsen IT**. 2013. Transcriptomic and biochemical
662 analyses identify a family of chlorhexidine efflux proteins. Proc Natl Acad Sci U S A
663 **110**:20254-9.

664 68. **Tattawasart U, Maillard JY, Furr JR, Russell AD**. 2000. Outer membrane changes in
665 *Pseudomonas stutzeri* resistant to chlorhexidine diacetate and cetylpyridinium chloride.
666 Int J Antimicrob Agents **16**:233-8.

bioRxiv preprint doi: https://doi.org/10.1101/148809; this version posted June 14, 2017. The copyright holder for this preprint (which was not certified by peer review) is the author/funder, who has granted bioRxiv a license to display the preprint in perpetuity. It is made available under aCC-BY-NC-ND 4.0 International license.

667 69. **Westergren G, Emilson CG**. 1980. In vitro development of chlorhexidine resistance in
668 *Streptococcus sanguis* and its transmissibility by genetic transformation. Scand J Dent
669 Res **88**:236-43.
670 70. **Guzman Prieto AM, Wijngaarden J, Braat JC, Rogers MR, Majoor E, Brouwer EC,**
671 **Zhang X, Bayjanov JR, Bonten MJ, Willems RJ, van Schaik W.** 2017. The two
672 component system ChtRS contributes to chlorhexidine tolerance in *Enterococcus*
673 *faecium*. Antimicrob Agents Chemother doi:10.1128/AAC.02122-16.
674 71. **Tally FP, Zeckel M, Wasilewski MM, Carini C, Berman CL, Drusano GL, Oleson FB**,
675 Jr. 1999. Daptomycin: a novel agent for Gram-positive infections. Expert Opin Investig
676 Drugs **8**:1223-38.
677 72. **Akins RL, Rybak MJ**. 2001. Bactericidal activities of two daptomycin regimens against
678 clinical strains of glycopeptide intermediate-resistant *Staphylococcus aureus*,
679 vancomycin-resistant *Enterococcus faecium*, and methicillin-resistant *Staphylococcus*
680 *aureus* isolates in an in vitro pharmacodynamic model with simulated endocardial
681 vegetations. Antimicrob Agents Chemother **45**:454-9.
682 73. **Alder JD.** 2005. Daptomycin: a new drug class for the treatment of Gram-positive
683 infections. Drugs Today (Barc) **41**:81-90.
684 74. **Munita JM, Murray BE, Arias CA**. 2014. Daptomycin for the treatment of bacteraemia
685 due to vancomycin-resistant enterococci. Int J Antimicrob Agents **44**:387-95.
686 75. **Muraih JK, Pearson A, Silverman J, Palmer M**. 2011. Oligomerization of daptomycin
687 on membranes. Biochim Biophys Acta **1808**:1154-60.
688 76. **Jung D, Rozek A, Okon M, Hancock RE**. 2004. Structural transitions as determinants
689 of the action of the calcium-dependent antibiotic daptomycin. Chem Biol **11**:949-57.
690 77. **Ho SW, Jung D, Calhoun JR, Lear JD, Okon M, Scott WR, Hancock RE, Straus SK**.
691 2008. Effect of divalent cations on the structure of the antibiotic daptomycin. Eur Biophys
692 J **37**:421-33.

bioRxiv preprint doi: https://doi.org/10.1101/148809; this version posted June 14, 2017. The copyright holder for this preprint (which was not certified by peer review) is the author/funder, who has granted bioRxiv a license to display the preprint in perpetuity. It is made available under aCC-BY-NC-ND 4.0 International license.

693 78. **Straus SK, Hancock RE**. 2006. Mode of action of the new antibiotic for Gram-positive
694 pathogens daptomycin: comparison with cationic antimicrobial peptides and
695 lipopeptides. Biochim Biophys Acta **1758**:1215-23.
696 79. **Muller A, Wenzel M, Strahl H, Grein F, Saaki TN, Kohl B, Siersma T, Bandow JE,**
697 **Sahl HG, Schneider T, Hamoen LW**. 2016. Daptomycin inhibits cell envelope synthesis
698 by interfering with fluid membrane microdomains. Proc Natl Acad Sci U S A **113**:E7077-
699 E7086.
700 80. **Bayer AS, Schneider T, Sahl HG**. 2013. Mechanisms of daptomycin resistance in
701 *Staphylococcus aureus*: role of the cell membrane and cell wall. Ann N Y Acad Sci
702 **1277**:139-58.
703 81. **Tran TT, Munita JM, Arias CA**. 2015. Mechanisms of drug resistance: daptomycin
704 resistance. Ann N Y Acad Sci **1354**:32-53.
705 82. **Mileykovskaya E, Dowhan W**. 2009. Cardiolipin membrane domains in prokaryotes
706 and eukaryotes. Biochim Biophys Acta **1788:**2084-91.
707 83. **Barak I, Muchova K**. 2013. The role of lipid domains in bacterial cell processes. Int J
708 Mol Sci **14**:4050-65.
709 84. **Tran TT, Panesso D, Mishra NN, Mileykovskaya E, Guan Z, Munita JM, Reyes J,**
710 **Diaz L, Weinstock GM, Murray BE, Shamoo Y, Dowhan W, Bayer AS, Arias CA.**
711 2013. Daptomycin-resistant *Enterococcus faecalis* diverts the antibiotic molecule from
712 the division septum and remodels cell membrane phospholipids. MBio **4**:e00281-13**.**
713 85. **Zorko M, Jerala R**. 2008. Alexidine and chlorhexidine bind to lipopolysaccharide and
714 lipoteichoic acid and prevent cell activation by antibiotics. J Antimicrob Chemother
715 **62**:730-7.
716 86. **Lee JK, Baik JE, Yun CH, Lee K, Han SH, Lee W, Bae KS, Baek SH, Lee Y, Son WJ,**
717 **Kum KY**. 2009. Chlorhexidine gluconate attenuates the ability of lipoteichoic acid from

bioRxiv preprint doi: https://doi.org/10.1101/148809; this version posted June 14, 2017. The copyright holder for this preprint (which was not certified by peer review) is the author/funder, who has granted bioRxiv a license to display the preprint in perpetuity. It is made available under aCC-BY-NC-ND 4.0 International license.

718 *Enterococcus faecalis* to stimulate toll-like receptor 2. J Endod **35**:212-5.

719 87. **Canepari P, Boaretti M, Lleo MM, Satta G.** 1990. Lipoteichoic acid as a new target for
720 activity of antibiotics: mode of action of daptomycin (LY146032). Antimicrob Agents
721 Chemother **34**:1220-6.

722 88. **Boaretti M, Canepari P, Lleo MM, Satta G**. 1993. The activity of daptomycin on
723 *Enterococcus faecium* protoplasts: indirect evidence supporting a novel mode of action
724 on lipoteichoic acid synthesis. J Antimicrob Chemother **31**:227-35.

725 89. **Laganas V, Alder J, Silverman JA**. 2003. In vitro bactericidal activities of daptomycin
726 against *Staphylococcus aureus* and *Enterococcus faecalis* are not mediated by inhibition
727 of lipoteichoic acid biosynthesis. Antimicrob Agents Chemother **47**:2682-4.

728 90. **Silverman JA, Perlmutter NG, Shapiro HM**. 2003. Correlation of daptomycin
729 bactericidal activity and membrane depolarization in *Staphylococcus aureus*. Antimicrob
730 Agents Chemother **47**:2538-44.

731 91. **Leenhouts K, Buist G, Bolhuis A, ten Berge A, Kiel J, Mierau I, Dabrowska M,**
732 **Venema G, Kok J**. 1996. A general system for generating unlabelled gene
733 replacements in bacterial chromosomes. Mol Gen Genet **253**:217-24.

bioRxiv preprint doi: https://doi.org/10.1101/148809; this version posted June 14, 2017. The copyright holder for this preprint (which was not certified by peer review) is the author/funder, who has granted bioRxiv a license to display the preprint in perpetuity. It is made available under aCC-BY-NC-ND 4.0 International license.

734 **Figure legends**

735

736 **Figure 1. *E. faecium* can adapt to CHX.** *In vitro* evolution of reduced CHX susceptibility in *E.*
737 *faecium* 1,231,410 (*E. faecium* 410) by serial passaging in increasing concentrations of CHX for
738 a period of 21 days. CHX passage MIC (y-axis) for each day of passage (x-axis) is shown for
739 two independent experiments (A and B).

740

741 **Figure 2. Reduced DAP susceptibility in CHX-passaged *E. faecium* populations A and B.**
742 The geometric mean and geometric standard deviation of CFU/ml count for n=3 or 4
743 independent trials is shown. Strains and populations are described in the text. The dashed line
744 represents limit of detection (10^3 CFU/ml). The boxed populations were sent for whole genome
745 sequencing. *, $P < 0.05$; one-tailed Student's *t* test.

746

747 **Figure 3. Cardiolipin levels are decreased in DAP-A1 and DAP-A2 mutants.** Lipidomic
748 analysis of *E. faecium* 410 and DAP strains DAP-A1 and -A2 was performed by normal-phase
749 LC-ESI/MS in the negative ion mode. The major lipids detected are phosphaditylglycerol (PG),
750 cardiolipin (CL), diacylglycerol (DAG), monohexosyldiacylglycerol (MHDAG),
751 dihexosyldiacylglycerol (DHDAG), phosphatidic acid (PA), and lysylphosphaditylglycerol (LPG).
752 While the PG levels are similar in all three strains, the CL levels are significantly decreased and
753 PA are increased in DAP-A1 and -A2 mutants compared to *E. faecium* 410. Shown are the total
754 ion chromatograms (TIC) and the selected mass spectra of $[M-H]^-$ ion species of PG and CL.

755

756 **Supplemental Figures and Tables**

757

758 **Figure S1. CHX induces *liaX* gene expression in *E. faecium*.** RT-qPCR was used to quantify

bioRxiv preprint doi: https://doi.org/10.1101/148809; this version posted June 14, 2017. The copyright holder for this preprint (which was not certified by peer review) is the author/funder, who has granted bioRxiv a license to display the preprint in perpetuity. It is made available under aCC-BY-NC-ND 4.0 International license.

759 the expression of *liaX* upon exposure to CHX for 15 min as compared to control untreated
760 condition. Expression of *liaX* was internally normalized to *clpX* and expression in control
761 cultures was set to 1 (not shown). The fold change in *liaX* expression in cultures treated with 1X
762 MIC CHX relative to the control was quantified for two independent (Trial 1 and 2) experiments.
763 Efm 410, *E. faecium* 1,231,410; Efm 733, *E. faecium* 1,141,733.

764

765 **Figure S2. *liaX* gene expression in DAP strains vs. parental strain.** RT-qPCR was used to
766 quantify the expression of *liaX* in the DAP strains at exponential phase (OD_{600}~0.6) vs. *E.*
767 *faecium* 410 wild-type in three independent trials. Expression of *liaX* was internally normalized
768 to *clpX* and *liaX* expression in control cultures was set to 1. The standard deviation was
769 calculated from n=3 independent experiments and one-tailed Student's *t*-test was used to
770 calculate significance value. *, $P < 0.05$. 410 wild-type, *E. faecium* 1,231,410.

771

772 **Figure S3. RT-qPCR for quantifying the expression levels of cytidylate kinase (*cmk*).** RT-
773 qPCR was used to quantify the expression of *cmk* in DAP mutant DAP-A1 and DAP-A2 vs. *E.*
774 *faecium* 410 during exponential growth (OD_{600} ~ 0.6). Expression of *cmk* was internally
775 normalized to *clpX*. Expression of *E. faecium* 410 *cmk* was set to 1 (not shown). The fold
776 change in *cmk* expression was quantified for two independent experiments.

777

778 **Figure S4. Quantification of intracellular organic phosphate (Pi) levels in *E. faecium* 410**
779 **wild-type and DAP-B1 mutant.** Intracellular Pi levels were measured for wild-type and DAP
780 strain DAP-B1 at different growth time points (OD_{600} 0.4-0.8) as described in materials and
781 methods. The levels (pmoles) were normalized using CFU count. Standard deviation was
782 calculated from n=3 independent experiments and significance value was calculated using one-
783 tailed Student's *t* test. Time points: 1, OD_{600} 0.4-0.5; 2, OD_{600} 0.5-0.6; 3, OD_{600} 0.6-0.7 and 4,
784 OD_{600} 0.7-0.8. *, $P < 0.05$. 410 wt, *E. faecium* 1,231,410.

bioRxiv preprint doi: https://doi.org/10.1101/148809; this version posted June 14, 2017. The copyright holder for this preprint (which was not certified by peer review) is the author/funder, who has granted bioRxiv a license to display the preprint in perpetuity. It is made available under aCC-BY-NC-ND 4.0 International license.

785

786 **Figure S5. Complementation of Δ*efrEF* deletion mutant.** The average CFU count of the
787 Δ*efrEF* deletion mutant transformed with empty pLZ12 vector and complementation vector
788 pAH201 on BHI and chloramphenicol plate supplemented with or without 1/8X MIC levels of
789 CHX from n=3 independent biological trials is shown. The CFU count was comparable for two
790 strains on BHI plate supplemented with chloramphenicol. A significantly higher CFU count of
791 Δ*efrEF* deletion mutant transformed with complementation vector was observed. *, $P < 0.05$
792 value was calculated using one-tailed Student's *t* test. Cam, chloramphenicol.

793

794 **Figure S6. Lipid-like compounds (Atmer-163) are detected in *E. faecium* 410 but not in**
795 **Δ*efrEF* mutant. A)** Positive ion ESI mass spectra showing the detection of Atmer-163 (C_{13})
796 ($[M+H]^+$ at *m/z* 288) and Atmer-163 (C_{15}) ($[M+H]^+$ ion at *m/z* 316) in *E. faecium* 410, and their
797 absence in the Δ*efrEF* mutant. **B**) Chemical structures and molecular formulae of Atmer-163
798 (C_{13}) and Atmer-163 (C_{15}). **C**) MS/MS spectrum of Atmer-163 (C_{15}) $[M+H]^+$ ion at *m/z* 316. The
799 fragment ion structures are depicted.

800

801 **Table S1.** List of primers used in the study.

802

803 **Table S2.** Doubling time and Rifampin mutation frequency for the DAP strains vs. *E. faecium*
804 410 wild-type.

805

806 **Table S3.** The relative levels of major lipids identified in *E. faecium* 410 wild-type and DAP
807 strains.

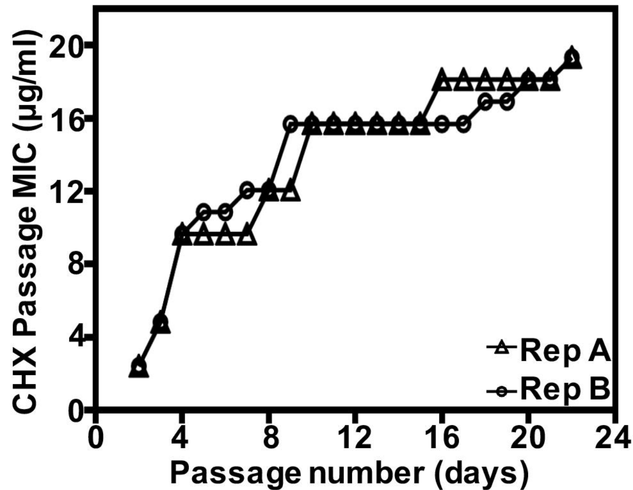
CHX Passage MIC (µg/ml)
0
4
8
12
16
20
Passage number (days)
0
4
8
12
16
20
24
Rep A
Rep B

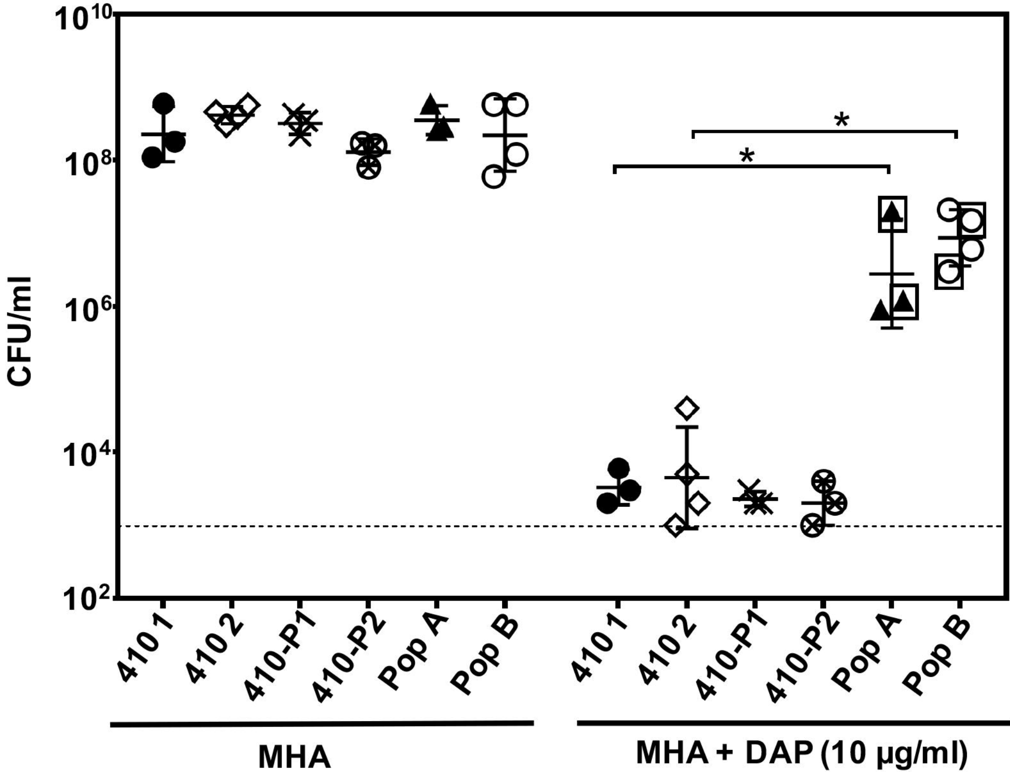

CFU/ml
10^10
10^8
10^6
10^4
10^2
*
*
410 1
410 2
410-P1
410-P2
Pop A
Pop B
410 1
410 2
410-P1
410-P2
Pop A
Pop B
MHA
MHA + DAP (10 µg/ml)

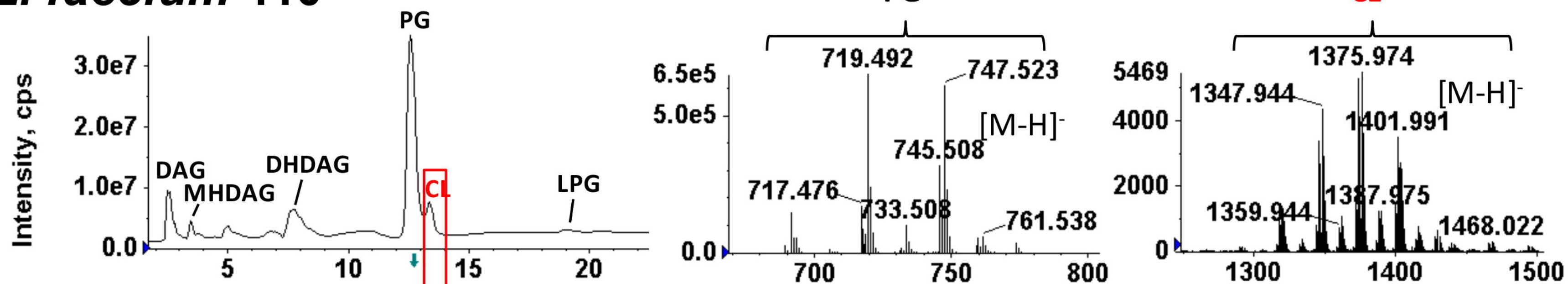
A) E. faecium 410
PG
CL
Intensity, cps
DAG
MHDAG
DHDAG
PG
CL
LPG
719.492
747.523
745.508
717.476
733.508
761.538
[M-H]-
1375.974
1347.944
1401.991
1387.975
1359.944
1468.022
[M-H]-

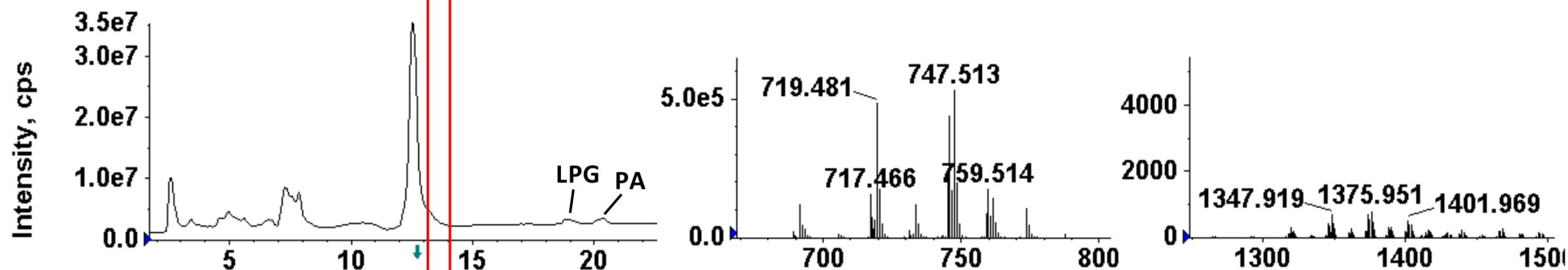
B) DAP-A1
Intensity, cps
LPG
PA
719.481
747.513
717.466
759.514
1347.919
1375.951
1401.969

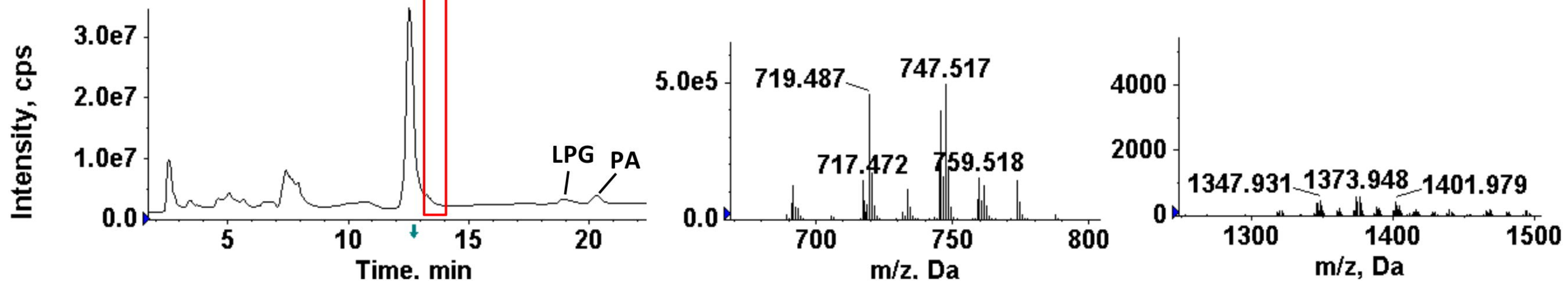
C) DAP-A2
Intensity, cps
LPG
PA
Time. min
719.487
747.517
717.472
759.518
m/z. Da
1347.931
1373.948
1401.979
m/z, Da